Prostagladin D_2 is a mast cell-derived antiangiogenic factor in lung carcinoma

Takahisa Murata[a,1], Kosuke Aritake[b], Shigeko Matsumoto[a], Shinya Kamauchi[b], Takayuki Nakagawa[c], Masatoshi Hori[a], Eiichi Momotani[d], Yoshihiro Urade[b], and Hiroshi Ozaki[a]

[a]Department of Veterinary Pharmacology and [c]Veterinary Surgery, Graduate School of Agriculture and Life Sciences, University of Tokyo, Tokyo 113-8657, Japan; [b]Department of Molecular Behavioral Biology, Osaka Bioscience Institute, Osaka 565-0874, Japan; and [d]Research Team for Paratuberculosis, National Institute of Animal Health, Tsukuba, Ibaraki 305-0856, Japan

Edited by Gregg L. Semenza, The Johns Hopkins University School of Medicine, Baltimore, MD, and approved October 27, 2011 (received for review June 23, 2011)

It is well established that prostaglandins (PGs) are involved in tumor angiogenesis and growth, yet the role of prostaglandin D_2 (PGD_2) remains virtually unknown. Here, we show that host hematopoietic PGD_2 synthase (H-PGDS) deficiency enhances Lewis lung carcinoma (LLC) progression, accompanied by increased vascular leakage, angiogenesis, and monocyte/mast cell infiltration. This deficiency can be rescued by hematopoietic reconstitution with bone marrow from H-PGDS–naive (WT) mice. In tumors on WT mice, c-kit$^+$ mast cells highly express H-PGDS. Host H-PGDS deficiency markedly up-regulated the expression of proangiogenic factors, including TNF-α in the tumor. In mast cell-null Kit$^{W\text{-}sh/W\text{-}sh}$ mice, adoptive transfer of H-PGDS–deficient mast cells causes stronger acceleration in tumor angiogenesis and growth than in WT mast cells. In response to LLC growth, H-PGDS–deficient mast cells produce TNF-α excessively. This response is suppressed by the administration of a synthetic PGD_2 receptor agonist or a degradation product of PGD_2, 15-deoxy-$\Delta^{12,14}$-PGJ_2. Additional TNF-α deficiency partially counteracts the tumorigenic properties seen in H-PGDS–deficient mast cells. These observations identify PGD_2 as a mast cell-derived antiangiogenic factor in expanding solid tumors. Mast cell-derived PGD_2 governs the tumor microenvironment by restricting excessive responses to vascular permeability and TNF-α production.

cancer | inflammation

Angiogenesis is crucial for both tumor progression and metastasis. Links between tumor angiogenesis and chronic inflammation have been well documented (1). As well as abnormally proliferating tumor cells, infiltrating hematopoietic lineage inflammatory cells, such as macrophages, lymphocytes, and mast cells, induce tumor angiogenesis by furnishing a variety of growth factors and cytokines (2). Thus, inflammatory cell infiltration has been well recognized as a crucial factor in tumor malignancy.

Epidemiological studies have provided evidence that nonsteroidal anti-inflammatory drugs that inhibit COX-dependent prostaglandin (PG) synthesis can significantly reduce the risk of cancer development (1). The main PGs responsible for tumor progression are currently being investigated. PGE_2 has already been shown to promote tumor growth and angiogenesis. Several groups have reported that the PGE_2-prostaglandin E receptor (EP) signal facilitates stromal VEGF expression, thus promoting tumor angiogenesis and growth (3, 4).

PGD_2 is another COX metabolite reported to promote sleep and to mediate inflammatory responses. There are two distinct isoforms of PGD_2 synthase, the hematopoietic-type (H-PGDS) and the lipocalin-type (L-PGDS). H-PGDS is a cytosolic protein responsible for the biosynthesis of PGD_2 in hematopoietic lineage cells, such as mast cells and Th2 lymphocytes (5). Thus, H-PGDS–derived PGD_2 is assumed to act mainly as an inflammatory mediator. In contrast, L-PGDS is a secretory protein mainly expressed in the central nervous system and is involved in sleep promotion (6).

The biological actions of PGD_2 are mediated through the G protein-coupled receptor, D prostanoid (DP), and the chemoattractant receptor-homologous molecule expressed on Th2 cells (CRTH2). Discrepancies exist regarding the proinflammatory or anti-inflammatory role of PGD_2 in pathophysiological conditions (5). Several studies demonstrate that DP signal activation inhibits the migration and activation of inflammatory cells (7, 8). Other groups have demonstrated that DP-deficient mice display decreased inflammatory responses to certain allergens (9), and that DP agonists produce conjunctival inflammation (10). CRTH2 is mainly expressed in inflammatory cells, and its activation has been consistently categorized as a proinflammatory signal. Furthermore, recent reports suggest that the dehydration product of PGD_2, 15-deoxy-^{12,14}-PGJ_2 (15d-PGJ_2), inhibits inflammatory responses via peroxisome proliferator-activated receptor-γ (PPAR-γ)–dependent or –independent signal activation (11). Thus, PGD_2 is likely to have a complex role by being both a pro- and anti-inflammatory mediator, depending on the target cell and stimulus.

In our previous study, we focused on the physiological function of PGD_2-DP signaling in the neovascular endothelial cells of expanding tumors, and found that stimulation of this pathway strongly tightens endothelial barriers and suppresses tumor angiogenesis (12). However, the pathophysiological implication of PGD_2 biosynthesis in tumors is virtually unexplored.

In the present study, we attempt to elucidate the contribution of PGD_2, derived from infiltrating cells of hematopoietic lineage, in tumor angiogenesis and growth. We demonstrate that infiltrating mast cells are the primary source of PGD_2, and that mast cell-derived PGD_2 suppresses vascular leakage and modulates TNF-α production, thus shaping the tumor microenvironment.

Results

Loss of Hematopoietic Cell-Derived PGD_2 Accelerates Tumor Growth. Lewis lung carcinoma (LLC) or B16 melanoma implanted onto the backs of H-PGDS–deficient (H-PGDS$^{-/-}$) mice grew faster than those implanted onto WT mice (Fig. 1*A* and Fig. S1*A*). Transplantation of H-PGDS–naive bone marrow (H-PGDS$^{-/-}$+WT^{HemRC}) reduced the increased rate of LLC growth on H-PGDS$^{-/-}$ mice to the same extent as for WT mice. Inversely, transplantation of H-PGDS$^{-/-}$ bone marrow (WT+H-PGDS$^{-/-HemRC}$) increased tumor malignancy in WT mice. Although abundant PGD_2 was detected in the tumors on WT and L-PGDS$^{-/-}$ mice (Fig. 1*B*), little was detected in the tumors on H-PGDS$^{-/-}$ mice. Tetranor-PGDM (11,15-deoxo-

Author contributions: T.M. and Y.U. designed research; T.M., K.A., S.M., S.K., and T.N. performed research; T.M., K.A., M.H., E.M., Y.U., and H.O. contributed new reagents/analytic tools; T.M., K.A., S.M., and S.K. analyzed data; and T.M. wrote the paper.

The authors declare no conflict of interest.

This article is a PNAS Direct Submission.

[1]To whom correspondence should be addressed. E-mail: amurata@mail.ecc.u-tokyo.ac.jp.

This article contains supporting information online at www.pnas.org/lookup/suppl/doi:10.1073/pnas.1110011108/-/DCSupplemental.

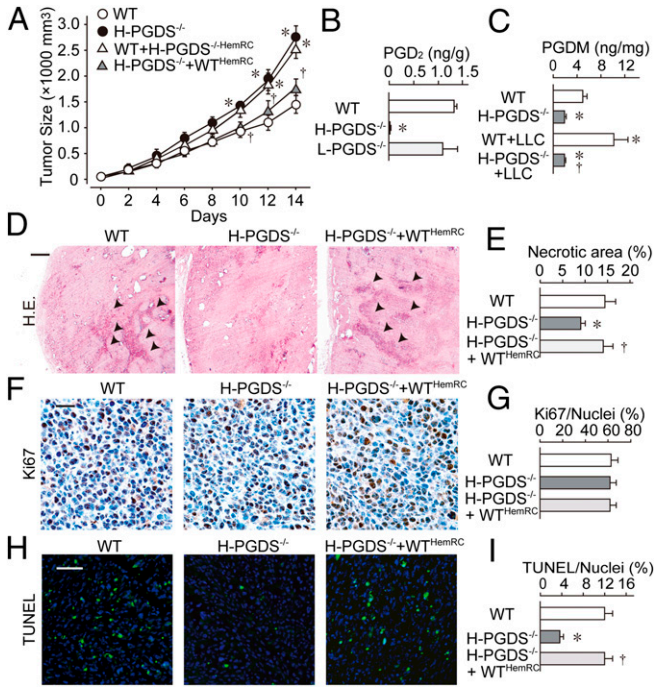

Fig. 1. (*A*) Tumors on H-PGDS$^{-/-}$ mice have increased growth rates (n = 25 each; $*^{\dagger}P < 0.05$ compared with WT or H-PGDS$^{-/-}$). (*B* and *C*) Detection of PGD_2 in implanted tumors and tetranor-PGDM in urine. The results were normalized to the weight of the tumor mass (*B*, n = 4 each) or normalized to creatinine content (*C*, n = 4–5; $*^{\dagger}P < 0.05$ compared with WT or WT+LLC). (*D–I*) Host H-PGDS deficiency decreases necrotic/apoptotic regions in tumors: H&E staining (*D*), Ki67 staining (*F*), or TUNEL (*H*). Ki67 staining (brown) was counterstained with hematoxylin (blue). (Scale bars: *D*, 200 μm; *F*, 10 μm; *H*, 50 μm.) TUNEL was counterstained with DAPI (blue) for nuclear labeling. Necrotic areas were quantified relative to total pixel density (*E*). The numbers of Ki67-positive or TUNEL-positive cells were normalized to total nuclei number (*G* and *I*, n = 6 each; $*^{\dagger}P < 0.05$ compared with WT or H-PGDS$^{-/-}$).

9a-hydroxy-2,3,4,5-tetranorprostan-1,20-dioic acid) is a stable metabolite in urine that indicates the biosynthesis of PGD_2 (13). We found that tumor growth boosted the excretion of tetranor-PGDM in WT mice (Fig. 1*C*), but in H-PGDS$^{-/-}$ mice its excretion was lower. These observations indicate H-PGDS is the main source of PGD_2 in tumors and suggest the possibility of urine tetranor-PGDM as a tumor marker.

H&E staining of tumor sections from WT mice revealed that commonly observed pockets of necrosis had spread more broadly throughout the tumor mass (Fig. 1*D*, arrowheads, day 14), which was in contrast to those seen in H-PGDS$^{-/-}$ mice, which had smaller necrotic areas (summarized in Fig. 1*E*). Hematopoietic reconstitution with WT bone marrow into H-PGDS$^{-/-}$ mice enlarged the area of necrosis. Tumor growth is the consequence of tumor-cell proliferation and apoptosis. As shown in Fig. 1*F*, neither H-PGDS deficiency nor hematopoietic reconstitution with WT bone marrow affected the number of proliferating Ki67^{+} cells (summarized in Fig. 1*G*). In contrast, TUNEL showed that tumors grown in H-PGDS$^{-/-}$ mice showed a decreased number of apoptotic cells (Fig. 1 *H* and *I*), which was completely corrected by hematopoietic reconstitution from WT mice. The reduction of tumor cell death under H-PGDS–deficiency was detected also as a decrease in leakage of a nonhistone nuclear factor, high-mobility group box 1 from nuclei (index of necrosis), or a caspase-3 cleavage (index of apoptosis) in tumor homogenates by Western blot (Fig. S1 *D–G*). These studies suggest that H-PGDS deficiency in hematopoietic lineage cells leads to a favorable environment for tumor growth by limiting tumor cell death.

H-PGDS Deficiency Increases Tumor Vascular Leakage and Angiogenesis. Similar to what has often been observed in solid tumors, LLC or B16 melanoma implanted into WT mice exhibit substantial angiogenesis [platelet endothelial cell adhesion molecule (PECAM-1)–staining] (Fig. 2*A* and Fig. S1*B*) and vascular leakage (fibrinogen deposition). Tumor sections from H-PGDS$^{-/-}$ mice revealed increased angiogenesis (summaries of staining, see Fig. 2*B* and Fig. S1*C*; VEGFR-2/Western blot, see Fig. S1 *H* and *I*) and vascular leakage (Fig. 2*C*). Hematopoietic reconstitution with WT bone marrow restored the increased immunopositivity scores. Furthermore, in comparison with that of WT mice, the tumor vasculature of H-PGDS$^{-/-}$ mice exhibited less coverage of smooth muscle actin (Fig. 2 *D* and *E*) or desmin (Fig. S1 *J* and *K*), indicating a less mature vasculature. Thus, our data support the concept that PGD_2 secreted from hematopoietic lineage cells reduces vascular leakage, angiogenesis, and tumor growth.

To determine whether H-PGD–dependent PGD_2 production can directly and acutely influence tumor vascular leakage, extravasation of Evans blue was monitored as a measure of albumin leakage. Fig. 2*F* demonstrates increased vascular permeability of tumors implanted on H-PGDS$^{-/-}$ mice compared with those on WT mice. Hematopoietic reconstitution from WT mice reduced the degree of hyperpermeability in the H-PGDS$^{-/-}$ mice tumors. Consistent with our previous observations that PGD_2 suppresses tumor hyperpermeability through DP activation, administration of the DP agonist BW245C (100 μg/kg, i.v., 10 min before dye infusion) strongly reduced dye extravasation both in WT and H-PGDS$^{-/-}$ mice tumors. These observations support the idea that PGD_2 originating from hematopoietic lineage cells is required for constitutive maintenance of tumor vascular barrier function.

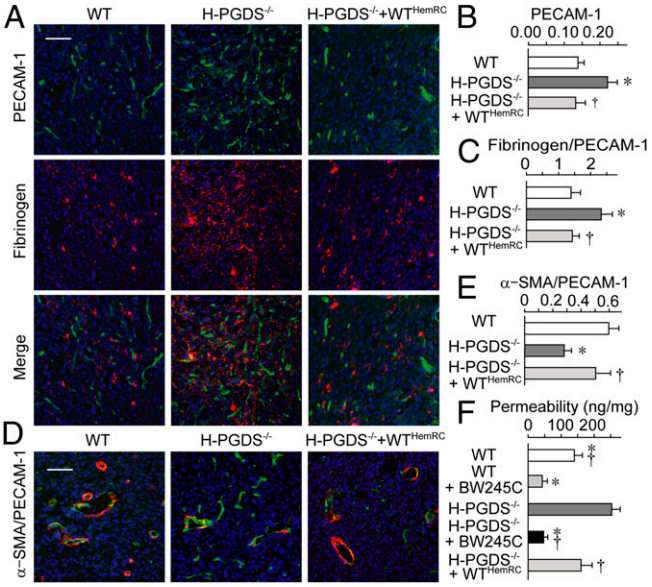

Fig. 2. H-PGDS–dependent PGD_2 production from bone marrow-derived cells decreases angiogenesis and vascular permeability in tumors. Tumor sections were subjected to immunostaining and then counterstained with DAPI (*A* and *D*) (Scale bars: *A* and *D*, 50 μm). Angiogenic area (PECAM-1) was quantified relative to total pixel density (*B*). Fibrinogen deposition was normalized to total PECAM-1^{+} pixel density (*C*, n = 6–10). The pixel density of α-SMA was normalized to total PECAM-1^{+} pixel density (*E*, n = 6 each). Dye extravasations (30 min) into tumor were quantified (*F*, n = 8 each). $*^{\dagger}P < 0.05$ compared with WT or H-PGDS$^{-/-}$.

PHARMACOLOGY

H-PGDS Deficiency Enhances Proangiogenic Properties in Tumors. We next examined the angiogenic properties of implanted tumors. As with hydron pellets that contain 100 ng VEGF, tumor pieces dissected from WT mice (day 10) and implanted into recipient mouse corneas showed extended neovasculature from the limbus (4 d after implantation) (Fig. 3 *A* and *B*). The tumor pieces dissected from H-PGDS$^{-/-}$ mice exhibited a robust increase (1.82-fold) in angiogenic response compared with that grown on WT. This increase was suppressed by the treatment of BW245C (5 μL of 0.35 ng/mL, twice a day) and 15d-PGJ$_2$ (5 μL of 0.2 ng/mL, twice a day), but not a CRTH2 agonist, 13,14-dihydro-15-keto-PGD$_2$ (DK-PGD$_2$; 5 μL of 0.3 ng/mL, twice a day). Consistently, the tumor pieces from H-PGDS$^{-/-}$+WT^{HemRC} mice reduced the increased tumor angiogenic capacity derived from H-PGDS$^{-/-}$ mice. Quantitative RT-PCR revealed that host H-PGDS deficiency increased proangiogenic gene expression of TNF-α, IL-6, moncyte chemoattractant protein-1 (MCP-1), VEGF-A, and TGF-β in the tumor (day 10, Fig. 3*C*). In particular, TNF-α expression was elevated almost fourfold in H-PGDS$^{-/-}$ mice. Hematopoietic reconstitution from WT mice lowered all of the elevated gene expressions observed in the tumors on H-PGDS$^{-/-}$ mice. Thus, PGD$_2$ originating from infiltrated hematopoietic lineage cells appears to modulate the production of proangiogenic factors in the tumor.

Mast Cells Express H-PGDS and TNF-α in the Expanding Tumor. Immunostaining was performed to determine which hematopoietic lineage cell expressed H-PGDS in the tumor. Although the blood cells labeled with anti-CD4, -8, -11b, -19, and -68 antibodies did not merge with the H-PGDS^{+} signal (CD68, Fig. 4*C*, and CD11b, -4, -8, Fig. S2 *A–C*, respectively), c-kit^{+} or FcεR1^{+} mast cells distinctively expressed H-PGDS (Fig. 4 *A* and *B*). Infiltrations of macrophage and mast cells are well recognized as being exacerbating factors of tumor growth. Interestingly, the number of CD68^{+} monocytes/macrophages (Fig. 4*D*, *Upper*) and mast cells (Fig. 4*D*, *Lower*), but not CD4^{-} or CD8^{+} cells (Fig. S2 *D* and *E*), were increased in tumors on H-PGDS$^{-/-}$ mice that were ameliorated by hematopoietic reconstitution from H-PGDS–naive donor mice. These observations suggest that host PGD$_2$ deficiency accelerates protumorigenic properties of the tumor microenvironment.

Next we attempted to detect the source of angiogenic factors whose mRNA expression levels were elevated in the tumors on H-PGDS$^{-/-}$ mice. As shown in Fig. 4*G*, c-kit^{+} mast cells strongly express TNF-α as well as PGD$_2$. MCP-1 was mainly detected in CD68^{+} monocyte/macrophage cells (Fig. 4*H*). In contrast, IL-6 and VEGF were broadly detected throughout the tumor mass (Fig. S2*F*).

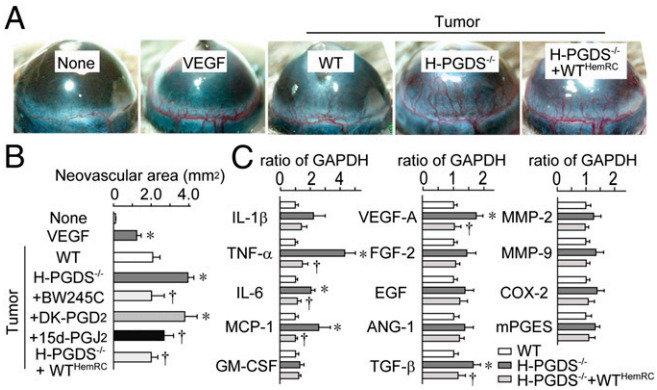

Fig. 3. (*A* and *B*) Host H-PGDS deficiency accelerates angiogenic properties of implanted tumors. Hydron pellets containing VEGF (100 ng) or tumor fractions (1.5 mm × 1.5 mm) were implanted into mice corneas. The corneal neovasculature was photographed (*A*), and quantified (*B*, n = 4–6). (*C*) Host H-PGDS deficiency accelerates mRNA expression of angiogenesis-related genes in implanted tumors. The data are represented as the ratio of WT (n = 5 each). $^{*\dagger}P < 0.05$ compared with WT or H-PGDS$^{-/-}$.

H-PGDS Deficiency Increases TNF-α Productivity of Bone Marrow-Derived Mast Cells. Isolated bone marrow cells proliferate/differentiate into mast cells by cultivation with IL-3. As shown in Fig. S3*A*, the cell-growth rates of WT and H-PGDS$^{-/-}$ bone marrow cells were identical. Five-week cultured H-PGDS$^{-/-}$ cells normally expressed both mast cell surface marker c-kit and FcεR1 (Fig. S3 *B* and *C*). As previously described (14), gene deficiency of TNF-α reduced the proliferation and c-kit^{high}FcεRI^{high} population of bone marrow cells (TNF-α$^{-/-}$ and H-PGDS$^{-/-}$TNF-α$^{-/-}$), that were rescued by a supplement with 1 ng/mL TNF-α. Thus, PGD$_2$ does not influence IL-3–mediated mast cell growth and differentiation in vitro, but TNF-α is required for it to occur.

We next measured the level of cytokine production for bone marrow-derived mast cells (BMMCs) (Fig. 5*A*). For WT BMMCs, antigenic stimulation [10 ng/mL dinitrophenyl-human serum albumin (DNP-HSA) for 24 h] elevated PGD$_2$ production, and LPS-stimulation (10 ng/mL for 24 h) elevated the production of PGD$_2$, TNF-α, and IL-6, but not VEGF. H-PGDS$^{-/-}$ BMMCs showed no PGD$_2$ production, but did secrete increased amounts of TNF-α and IL-6, regardless of the kind of stimulation. It is particularly notable that for TNF-α production, H-PGDS$^{-/-}$ BMMCs showed a more than twofold increase compared with WT BMMCs for both stimulatory regimens. Additional gene disruption of TNF-α (H-PGDS$^{-/-}$TNF-α$^{-/-}$) reduced the increased level of IL-6 production seen for H-PGDS$^{-/-}$ BMMCs. Both H-PGDS$^{-/-}$TNF-α$^{-/-}$ and TNF-α$^{-/-}$ BMMCs produced significantly less IL-6 than WT BMMCs in response to LPS-stimulation, suggesting a TNF-α–dependency for IL-6 production. These in vitro observations suggest that an H-PGDS deficiency enhances the protumorigenic properties of mast cells by elevating the level of TNF-α production.

Mast Cell-Derived PGD$_2$ Attenuates Tumor Expansion. Kit$^{W\text{-}sh/W\text{-}sh}$ mice lack mature mast cells because of an inversion mutation in the Kit gene promoter. In Kit$^{W\text{-}sh/W\text{-}sh}$ mice, implanted tumors grew slower than that in WT mice (Fig. 5*B*). In tumors on Kit$^{W\text{-}sh/W\text{-}sh}$ mice, a significantly lower amount of PGD$_2$ was detected compared with that on WT mice (WT: 1,311.5 ± 23.1 pg/g; Kit$^{W\text{-}sh/W\text{-}sh}$: 289.6 ± 21.3 pg/g, day 14, $P < 0.05$, n = 5 each), thus providing evidence that mast cells are the primary source of PGD$_2$ in the implanted tumor. Adoptive transfer of syngeneic WT BMMCs (Kit$^{W\text{-}sh/W\text{-}sh}$+WT^{BMMC}) successfully redistributed the mast cells into the implanted tumors (Fig. S4*C*) and increased the tumor growth rate on Kit$^{W\text{-}sh/W\text{-}sh}$ mice to that seen on mast cell naive WT mice (Fig. 6*A*). Reconstitution of H-PGDS$^{-/-}$ mast cells (Kit$^{W\text{-}sh/W\text{-}sh}$+H-PGDS$^{-/-BMMC}$) exhibited a further acceleration of tumor expansion even greater than that seen on WT mast cells (Fig. 5*C*).

We next examined the role of TNF-α in the tumorigenic properties of H-PGDS$^{-/-}$ mast cells. As shown in Fig. 5*C*, additional gene disruption of TNF-α (Kit$^{W\text{-}sh/W\text{-}sh}$+H-PGDS$^{-/-}$TNF-α$^{-/-BMMC}$) reduced the increased rate of tumorigenesis observed in Kit$^{W\text{-}sh/W\text{-}sh}$+H-PGDS$^{-/-BMMC}$ mice. However, the tumor growth rate for Kit$^{W\text{-}sh/W\text{-}sh}$+H-PGDS$^{-/-}$TNF-α$^{-/-BMMC}$ mice was still higher than that for Kit$^{W\text{-}sh/W\text{-}sh}$+TNF-α$^{-/-BMMC}$ mice. These data provide direct evidence of a critical role for mast cell-derived PGD$_2$ and TNF-α on tumor expansion in vivo. Furthermore, the data suggest that TNF-α somehow mediates the accelerated tumorigenic properties of H-PGDS$^{-/-}$ mast cells.

Mast Cell-Derived PGD$_2$ Attenuates Tumor Angiogenesis. Consistent with blunted tumor growth, tumors (day 14) on Kit$^{W\text{-}sh/W\text{-}sh}$ mice exhibited a reduced number of endothelial cells (Fig. 5*D*),

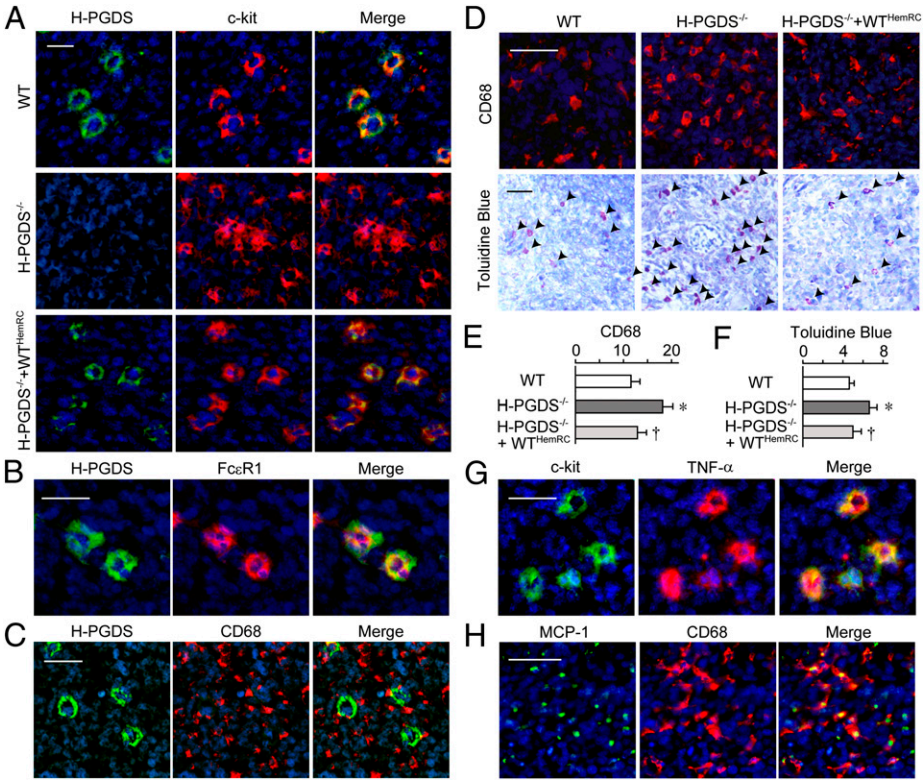

Fig. 4. Mast cells express H-PGDS and produce TNF-α (*A–C*, *G*), and monocyte/macrophages produce MCP-1 (*H*). Sections were stained for H-PGDS and c-kit (*A*), H-PGDS and FcεR1 (*B*), H-PGDS and CD68 (*C*), c-kit and TNF-α (*G*), or MCP-1 and CD68 (*H*) with counterstaining with DAPI. (*D–F*) H-PGDS deficiency accelerates monocyte- and mast cell-infiltration into the tumor. Sections were labeled for CD68 (*D*, *Upper*) or Toluidine blue (*D*, *Lower*) (Scale bars, 50 μm). The number of stained cells was normalized to field area (*E* and *F*, n = 6 each). $*^{\dagger}P < 0.05$ compared with WT or H-PGDS$^{-/-}$.

decreased levels of fibrinogen deposition (Fig. 5*E*), and monocyte/macrophage infiltration (Fig. 5*G*) compared with the WT controls (Figs. 2 *B* and *C*, and Fig. 4*E*). Adoptive transfer of syngeneic WT mast cells (Kit$^{W\text{-}sh/W\text{-}sh}$+WT^{BMMC}) boosted these histological scores, identifying the role of mast cells in exacerbating tumor growth. Tumors on mast cell-specific H-PGDS$^{-/-}$ mice showed a further increase in histological scores similar to those seen with systemic H-PGDS$^{-/-}$ mice (Fig. 5 *D–H*). An additional gene deficiency of TNF-α (Kit$^{W\text{-}sh/W\text{-}sh}$+H-PGDS$^{-/-}$TNF-α$^{-/-BMMC}$) partially reduced the enhanced scores seen in Kit$^{W\text{-}sh/W\text{-}sh}$+H-PGDS$^{-/-BMMC}$ mice, excepting that for tumor permeability. Tumors with TNF-α$^{-/-}$ mast cells (Kit$^{W\text{-}sh/W\text{-}sh}$+TNF-α$^{-/-BMMC}$) showed lower scores than those for WT mast cells.

As shown in Fig. 6*A*, gene analysis revealed that a mast cell deficiency (Kit$^{W\text{-}sh/W\text{-}sh}$) diminished the expression of proangiogenic factors in implanted tumors and that expression was restored by reconstitution with WT mast cells. As expected, H-PGDS$^{-/-}$ mast cells (Kit$^{W\text{-}sh/W\text{-}sh}$+H-PGDS$^{-/-BMMC}$) enhanced the level of mRNA expression of four proangiogenic factors, TNF-α, IL-6, MCP-1, and VEGF-A, in the tumor. In particular, TNF-α expression in H-PGDS$^{-/-}$ mast cells showed a 1.7-fold increase compared with WT mast cells. Additional gene disruption of TNF-α (Kit$^{W\text{-}sh/W\text{-}sh}$+H-PGDS$^{-/-}$TNF-α$^{-/-BMMC}$) partially counteracted the elevated expression of TNF-α and IL-6, but not of MCP-1 or VEGF-A observed in tumors on Kit$^{W\text{-}sh/W\text{-}sh}$+H-PGDS$^{-/-BMMC}$ mice. The mRNA expression levels of these four genes were reduced in tumors on Kit$^{W\text{-}sh/W\text{-}sh}$+TNF-α$^{-/-BMMC}$ mice. These observations suggest that mast cell-derived PGD_2 exhibits antiangiogenic properties at least partially by inhibiting the production of TNF-α in mast cell itself.

PGD_2 Modulates Angiogenic Properties in Tumor-Educated Mast Cells. When LLC cells are injected intraperitoneally, they attach at multiple locations to form sites for tumor development with the subsequent development of ascites. Differentiation/infiltration of mast cells into the peritoneal cavity was significantly higher in H-PGDS$^{-/-}$ mice than in WT mice (Fig. 6*C*). Whereas nonstimulated mast cells isolated from the abdominal cavity of WT mice distinctively express TNF-α, peritoneal inoculation of LLC cells (14 d) further boosted TNF-α expression (Fig. 6*B*). Thus, this procedure allows us to identify the characteristic changes in tumor-educated mast cells. As expected, gene expression of TNF-α and IL-6 was enhanced in H-PGDS$^{-/-}$ peritoneal mast cells in response to LLC tumor growth. This enhancement was eliminated when the gene expressing TNF-α was disrupted. Interestingly, H-PGDS deficiency did not influence the expression of other proangiogenic genes (MCP-1, VEGF-A, and TGF-β) in mast cells, which were increased in the tumors on H-PGDS$^{-/-}$ mice (Fig. 3*C*).

We next investigated the mechanisms underlying the excessive activation of H-PGDS$^{-/-}$ mast cells against tumor growth. As shown in Fig. 6 *C* and *D*, concomitant administration of the DP receptor agonist BW245C (100 μg/kg, twice a day), 15d-PGJ_2 (30 μg/kg, twice a day), and troglitazone, a synthetic PPAR-γ activator (Trogli: 300 μg/kg, twice a day) significantly reduced elevated infiltration, TNF-α expression, and IL-6 expression seen in H-PGDS$^{-/-}$ mast cells. However, the administration of a CRTH2 agonist, DK-PGD_2 (100 μg/kg, twice a day), did not show any effects. Similar results were obtained in 10 ng/mL LPS-induced TNF-α production in BMMCs (Fig. S4*D*). These findings suggest that the mast cell automodulates its own angiogenic/inflammatory properties via H-PGDS–dependent PGD_2 production into the expanding tumor. DP receptor activation and PGJ_2-PPAR-γ–mediated anti-inflammatory reactions are involved in this autoregulatory system.

Discussion

In this study, we investigate the role of H-PGDS–derived PGD_2 on implanted LLC growth. Although it is well established that mast cells abundantly produce PGD_2, there is no direct evidence showing the participation of PGD_2 in tumorigenesis. Here, we

PHARMACOLOGY

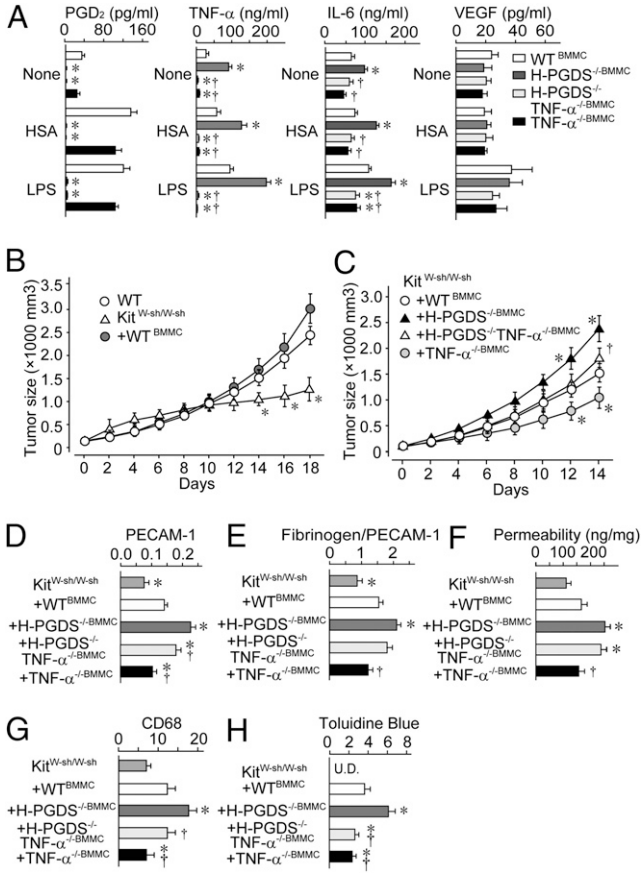

Fig. 5. (*A*) H-PGDS deficiency accelerates TNF-α production of BMMC (n = 6–8). Mast cell-specific H-PGDS deficiency accelerates tumor growth (*B* and *C*, n = 15–20) by altering angiogenesis (*D*), vascular permeability (*E* and *F*), monocyte infiltration (*G*), and mast cell infiltration (*H*). Tumor sections were subjected to immunostaining or Toluidine blue staining. Angiogenic areas (PECAM-1) were quantified relative to total pixel density (*D*). Fibrinogen deposition was normalized to total PECAM-1$^+$ pixel density (*E*, n = 6–10). The number of CD68$^+$ cells or metachromatically stained cells was normalized to field area (*G* and *H*, n = 6 each). (*F*) Dye extravasations (30 min) into tumor were quantified (n = 8 each). $*^{\dagger}P < 0.05$ compared with Kit$^{W\text{-}sh/W\text{-}sh}$+WT^{BMMC} mice or Kit$^{W\text{-}sh/W\text{-}sh}$+H-PGDS$^{-/-BMMC}$ mice.

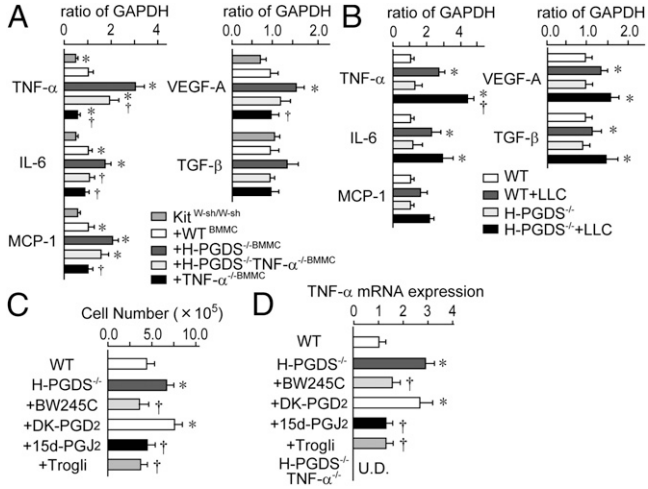

Fig. 6. (*A*) Mast cell-specific H-PGDS deficiency accelerates angiogenesis-related gene expression in tumor (day 14). The data are represented as the ratio of Kit$^{W\text{-}sh/W\text{-}sh}$+WT^{BMMC} ($n$ = 8 each; $*^{\dagger}P < 0.05$ compared with Kit$^{W\text{-}sh/W\text{-}sh}$+WT^{BMMC} mice or Kit$^{W\text{-}sh/W\text{-}sh}$+H-PGDS$^{-/-BMMC}$ mice). (*B–D*) H-PGDS deficiency accelerates and DP agonism or PGJ$_2$ attenuates mast cell infiltration and its TNF-α/IL-6 expression in response to tumor implantation. Three weeks after the injection of tumor the numbers of peritoneal mast cells were counted (*B*, n = 6–9). The data of mRNA expressions are represented as the ratio of WT (*C* and *D*, n = 6 each; $*^{\dagger}P < 0.05$ compared with WT or H-PGDS$^{-/-}$).

identify mast cell-derived PGD$_2$ as a unique antiangiogenic mediator in actively growing lung carcinoma.

Epidemiological studies have provided evidence that inhibition of COX-2–dependent prostaglandin synthesis can reduce the risk of cancer development in various types of cancer (1). Furthermore, experimental studies have reported that major prostaglandins, PGE$_2$ and thromboxane A$_2$ represents proangiogenic/tumorigenic properties (3, 4, 15). These studies strongly support the idea that COX-2 activation is protumorigenic as a whole. In contrast, we showed PGD$_2$-signal acts as an antitumorigenic factor in a mouse model. The other groups also suggested enhancement of PGI$_2$ signal protect against lung carcinoma growth and metastasis (15, 16). Thus, COX and its metabolites appear to be related to tumor development through multiple mechanisms.

Although mast cells have been found to accumulate around various types of solid tumors, the link between mast cell invasion and tumor malignancy has also been an area of controversy (17). Several epidemiological studies suggest a correlation between the presence of mast cells and a poor prognosis in human tumors, such as melanoma and prostate cancer. Other studies suggest a correlation between the presence of mast cells and a good prognosis in breast cancer and ovarian cancer. On the other hand, a majority of experimental studies have shown that mast cells act as critical upstream regulators of numerous types of inflammatory cells and secrete several mediators, including heparin, TNF-α, and VEGF, all of which contribute to various aspects of neovascularization (18). Here we showed that mast cell-derived PGD$_2$ is a negative regulator of tumor angiogenesis and growth. These observations indicate dual roles for the mast cell in tumor growth, one being antitumorigenic and the other protumorigenic. Of interest, Maltby et al. suggested the possibility that tumor may somehow educate mast cells and convert their phenotype during development (18). PGD$_2$ signal might be a useful phenotypic modulator of mast cells to prevent, or at least slow, tumor development.

Because of their rapid growth, newly sprouting vessels in tumors are usually very immature and highly leaky (19). Vascular leakage is the first angiogenic response of peripheral vessels to VEGF, and the resulting extravasation of plasma proteins support endothelial and tumor cell growth. Thus, investigators assume its restriction can be applied to anticancer therapy. We previously showed that the PGD$_2$ receptor DP is abundantly expressed in the neovascular endothelial cell and its deficiency loosens the vascular barrier in tumors (12). Loss of DP signal-mediated vascular barrier protection is at least partially responsible for tumor malignancy observed in H-PGDS–deficient models. Additionally, our data showed that mast cell-derived PGD$_2$ reduces its own TNF-α synthesis, and then restricts protumorigenic responses in the microenvironment. Evidence has accumulated indicating endogenous TNF-α signaling is a strong contributing factor to protumorigenic changes in the tumor microenvironment. Gene disruption of TNF-α promote resistance to skin carcinogenesis (20). Treatment with anti–TNF-α antibodies reduced polyp growth and decreased mast cell infiltration in an adenomatous polyp model (21). Because various types of cells other than mast cells are assumed to secrete TNF-α in tumors, mast cell-derived PGD$_2$ may also modulate TNF-α production in neighboring cells.

Treatment with 15d-PGJ$_2$, as well as a DP agonist, corrected the increased tumorigenic properties seen under H-PGDS–deficient conditions. The degraded product of PGD$_2$, 15d-PGJ$_2$, is currently thought to inhibit inflammation both through PPAR-γ–dependent or –independent signaling pathways (11). However, it

is still uncertain whether enough degraded 15d-PGJ_2 is present to produce the observed pathology in vivo. Further investigation is needed to explore the roles of PGJ_2 in tumorigenesis.

In this study, we identified PGD_2 as a mast cell-derived anti-angiogenic factor in the growing tumor. Mast cell-derived PGD_2 restricts its own abnormal production of TNF-α and vascular hyperpermeability, thus governing inflammatory response in the tumor microenvironment. Mast cells are often observed in the skin, airway, and perivascular area of tissues in human body, and its activation is involved in the progression of tissue inflammation and cardiovascular events, through the production of a variety of cytokines (22). Inhibition of mast cell activity by PGD_2-signal enhancement might be useful for future management of these diseases as well as tumor malignancy.

Materials and Methods

LLC Transplantation. All experiments were approved by the institutional animal care and use committees of The University of Tokyo. H-PGDS$^{-/-}$ or TNF-α$^{-/-}$ mice (C57BL/6J-background) were generated and bred as previously described (23, 24). Mast cell-deficient Kit$^{W\text{-}sh/W\text{-}sh}$ mice were kindly provided by RIKEN BRC, Japan. For bone marrow reconstitution, 5-wk-old male mice received 9 Gy of irradiation for bone marrow ablation. Bone marrow cells (2×10^6) freshly isolated from donor mice were injected into the tail vein of the recipient. Eight weeks after transplantation, the mice were used for the experiments. LLC cells (1×10^6 cells) were injected subcutaneously on the backs of mice. Tumor size was determined by applying the formula to approximate the volume of a spheroid [$0.52 \times (\text{width})^2 \times (\text{length})$].

Preparation of BMMCs and Adoptive Transfer to Kit$^{W\text{-}sh/W\text{-}sh}$ Mice. To prepare BMMCs, bone marrow cells were cultured with 10% (vol/vol) FBS, 10 ng/mL IL-3, and 50 μM 2-mercaptoethanol for 5–7 wk. BMMCs were transferred via intradermal injection (5×10^6 cells in 6×50-μL aliquots in three rows down the length of the back of mouse) and via tail-vein injection (5×10^6 cells) into a 5-wk-old Kit$^{W\text{-}sh/W\text{-}sh}$ mouse. Eight weeks postinjection, mast cells were redistributed to the back skin and lung of Kit$^{W\text{-}sh/W\text{-}sh}$ mice (Fig. S4 *A* and *B*, respectively), then mice were applied for LLC injection. Additionally, BMMCs (1×10^6) were transferred via tail-vein injection every 5 d after LLC transplantation.

Tumor-Associated Mast Cell Isolation. For tumor-associated mast cell isolation, 5×10^6 LLCs were injected into the mouse peritoneal cavity. Three weeks after that, mast cells were isolated from a suspension of mouse peritoneal cells using a 40% Percoll density gradient. More than 96% of the isolated cells were metachromatically stained with Toluidine blue. Intraperitoneal treatments with BW245C, 13,14-dihydro-15-keto-PGD_2, 15d-PGJ_2 (Cayman Chemicals), or Troglitazone (Sigma-Aldrich) were started 2 wk after the LLC injection.

PGD_2 or Tetranor-PGDM Measurements. For PGD_2 measurement, tumors were homogenized in ethanol containing 0.02% HCl, and the samples were separated by HPLC. Quantification was performed using a PGD_2-MOX EIA kit (Cayman Chemicals). For tetranor-PGDM measurement, collected mouse urines were separated by HPLC. A API3200 triple-quadruple tandem mass spectrometer (Applied Biosystems) was used.

Stainings. Paraffin-embedded sections were used for H&E, Toluidine blue, and Ki67 staining. Cryosections were used for all other staining. The primary antibodies used were anti-Ki67 (Santa Cruz), H-PGDS (Cayman Chemicals), α-SMA, CD4, CD8, CD11b, CD19, CD31 (BD Biosciences), fibrinogen (DAKO), CD68 (Serotec), TNF-α (R&D Systems), and c-kit (Merck Chemical) antibodies. For apoptotic cell labeling, a TUNEL assay kit (Roche) was used.

Tumor Permeability. Tumors were grown to ~800–1,000 mm^3. Evans blue (30 mg/kg) was injected through the tail vein and circulated for 30 min. Evans blue extravasated into tumor mass was extracted in formamide and its content was quantified by reading at 610 nm in a spectrophotometer.

Corneal Micropocket Assay. Hydron pellets containing VEGF (Sigma-Aldrich) or tumor fractions (~1.5 mm × 1.5 mm, day 10) were implanted in murine corneas. Four or 6 d after implantation, corneal vessels were photographed and areas of neovascularization were analyzed using ImageJ 1.37.

Quantitative RT-PCR. Total RNA was reverse-transcribed into cDNA. Subsequent real-time PCR using platinum SYBR Green qPCR SuperMix-UDG (Invitrogen) and specific primers (Table S1) was performed.

Flow Cytometric Analysis. Flow cytometric analysis was performed with an anti-c-kit and anti-FcεRI antibodies (Biolegend).

Cytokine Measurements for BMMCs. After overnight incubation with 50 ng/mL anti-DNP IgE (Sigma-Aldrich), BMMCs (1×10^6 cells) were stimulated with 10 ng/mL DNP-HSA or 10 ng/mL LPS for 24 h. The supernatants were analyzed using EIAs for TNF-α, IL-1b, IL-6 (R&D Systems) and PGD_2 (Cayman).

Data Representation. All data are shown as mean ± SEM. The statistical difference was determined by Student *t* test for two-group comparison, by one-way ANOVA with Dunnett's test for multiple group comparison, or two-way ANOVA with Bonferroni test for comparison of tumor growth rates.

ACKNOWLEDGMENTS. This work was supported by Grant-in-Aid for Young Scientists (A) from the Japan Society for the Promotion of Science, the Yasuda Medical Foundation, the Foundation for Promotion of Cancer Research, and the Sagawa Foundation.

1. Coussens LM, Werb Z (2002) Inflammation and cancer. *Nature* 420:860–867.
2. Murdoch C, Muthana M, Coffelt SB, Lewis CE (2008) The role of myeloid cells in the promotion of tumour angiogenesis. *Nat Rev Cancer* 8:618–631.
3. Amano H, et al. (2003) Host prostaglandin E(2)-EP3 signaling regulates tumor-associated angiogenesis and tumor growth. *J Exp Med* 197:221–232.
4. Shao J, Sheng GG, Mifflin RC, Powell DW, Sheng H (2006) Roles of myofibroblasts in prostaglandin E2-stimulated intestinal epithelial proliferation and angiogenesis. *Cancer Res* 66:846–855.
5. Kostenis E, Ulven T (2006) Emerging roles of DP and CRTH2 in allergic inflammation. *Trends Mol Med* 12:148–158.
6. Qu WM, et al. (2006) Lipocalin-type prostaglandin D synthase produces prostaglandin D2 involved in regulation of physiological sleep. *Proc Natl Acad Sci USA* 103:17949–17954.
7. Monneret G, Gravel S, Diamond M, Rokach J, Powell WS (2001) Prostaglandin D2 is a potent chemoattractant for human eosinophils that acts via a novel DP receptor. *Blood* 98:1942–1948.
8. Spik I, et al. (2005) Activation of the prostaglandin D2 receptor DP2/CRTH2 increases allergic inflammation in mouse. *J Immunol* 174:3703–3708.
9. Matsuoka T, et al. (2000) Prostaglandin D2 as a mediator of allergic asthma. *Science* 287:2013–2017.
10. Hellberg MR, et al. (2002) 3-Oxa-15-cyclohexyl prostaglandin DP receptor agonists as topical antiglaucoma agents. *Bioorg Med Chem* 10:2031–2049.
11. Scher JU, Pillinger MH (2005) 15d-PGJ2: The anti-inflammatory prostaglandin? *Clin Immunol* 114:100–109.
12. Murata T, et al. (2008) Role of prostaglandin D2 receptor DP as a suppressor of tumor hyperpermeability and angiogenesis in vivo. *Proc Natl Acad Sci USA* 105:20009–20014.
13. Song WL, et al. (2008) Tetranor PGDM, an abundant urinary metabolite reflects biosynthesis of prostaglandin D2 in mice and humans. *J Biol Chem* 283:1179–1188.
14. Wright HV, et al. (2006) IL-3-mediated TNF production is necessary for mast cell development. *J Immunol* 176:2114–2121.
15. Pradono P, et al. (2002) Gene transfer of thromboxane A(2) synthase and prostaglandin I(2) synthase antithetically altered tumor angiogenesis and tumor growth. *Cancer Res* 62:63–66.
16. Cuneo KC, Fu A, Osusky KL, Geng L (2007) Effects of vascular endothelial growth factor receptor inhibitor SU5416 and prostacyclin on murine lung metastasis. *Anticancer Drugs* 18:349–355.
17. Ribatti D, Crivellato E (2009) The controversial role of mast cells in tumor growth. *Int Rev Cell Mol Biol* 275:89–131.
18. Maltby S, Khazaie K, McNagny KM (2009) Mast cells in tumor growth: Angiogenesis, tissue remodelling and immune-modulation. *Biochim Biophys Acta* 1796:19–26.
19. McDonald DM, Baluk P (2002) Significance of blood vessel leakiness in cancer. *Cancer Res* 62:5381–5385.
20. Moore RJ, et al. (1999) Mice deficient in tumor necrosis factor-alpha are resistant to skin carcinogenesis. *Nat Med* 5:828–831.
21. Gounaris E, et al. (2007) Mast cells are an essential hematopoietic component for polyp development. *Proc Natl Acad Sci USA* 104:19977–19982.
22. Abraham SN, St John AL (2010) Mast cell-orchestrated immunity to pathogens. *Nat Rev Immunol* 10:440–452.
23. Mohri I, et al. (2006) Prostaglandin D2-mediated microglia/astrocyte interaction enhances astrogliosis and demyelination in twitcher. *J Neurosci* 26:4383–4393.
24. Kaneko H, et al. (1999) Role of tumor necrosis factor-alpha in Mycobacterium-induced granuloma formation in tumor necrosis factor-alpha-deficient mice. *Lab Invest* 79:379–386.

Supporting Information

Murata et al. 10.1073/pnas.1110011108

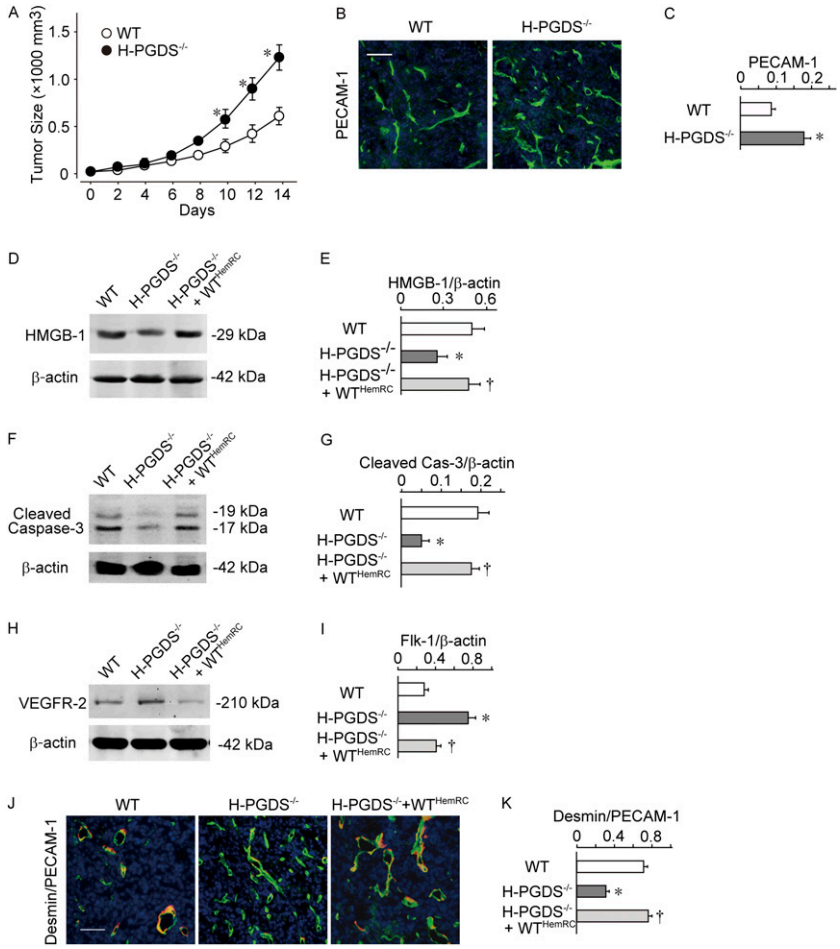

Fig. S1. (*A*–*C*) Host hematopoietic prostaglandin D_2 (PGD_2) synthase (H-PGDS) deficiency accelerates tumor growth and angiogenesis in B16 melanoma. Melanoma cells (1×10^6) were injected subcutaneously on the backs of mice, and tumor growth was monitored (*A*, $n = 8$ each). Tumor sections (day 14) were labeled with anti–PECAM-1 (platelet endothelial cell adhesion molecule) antibody (*B*) and the labeled area was quantified relative to total pixel density (*C*, $n = 8$ each). (Scale bar in *B*, 50 μm.) (*D*–*I*) Absence of bone marrow-derived PGD_2 decreases necrotic/apoptotic cell death, and increases angiogenesis in growing Lewis lung carcinoma (LLC) tumor. Cytoplasmic proteins extracted from tumor mass (day 14) were applied for Western blot to detect the high mobility group box 1 (HMGB-1) protein leakage from nuclei. Total protein extracts were applied to detect cleaved caspase-3 or an endothelial marker, VEGFR-2. Band intensities were normalized and shown as the ratio of β-actin ($n = 5$ each). Anti–HMGB-1, cleaved caspase-3 (Cell Signaling), VEGFR-2 (R&D Systems), and β-actin (Sigma-Aldrich) antibodies were used. (*J* and *K*) Host H-PGDS deficiency decreases pericyte-coverage in the tumor-neovasculature. Tumor sections were labeled with antidesmin antibody (Abcam) and anti–PECAM-1 antibody (*J*) (Scale bar, 50 μm). The pixel density of desmin was normalized to total PECAM-1$^+$ pixel density (*K*, $n = 5$ each). Results are expressed as means ± SEM. $*^{\dagger}P < 0.05$ compared with WT or H-PGDS$^{-/-}$, respectively.

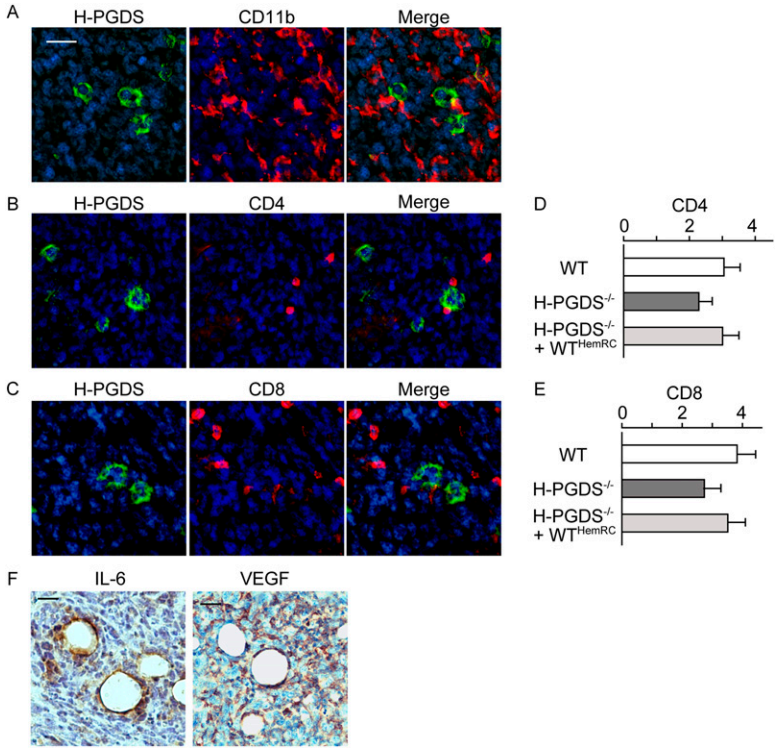

Fig. S2. (*A–E*) Infiltrating CD11b$^+$, CD4$^+$, or CD8$^+$ cells do not express H-PGDS in tumors. Sections were subjected to double immunostaining for H-PGDS and CD11b (*A*) , H-PGDS and CD4 (*B*), or H-PGDS and CD8 (*C*). (Scale bar in A, 50 μm.) Their numbers were normalized to field area (*D* and *E*, results are expressed as means ± SEM, $n = 6$ each). (*F*) Expression of IL-6 or VEGF in tumor. Paraffin-embedded sections of tumor on WT mice were labeled with anti–IL-6 (Santa Cruz) or anti-VEGF (Sigma-Aldrich) antibodies (Scale bars, 50 μm).

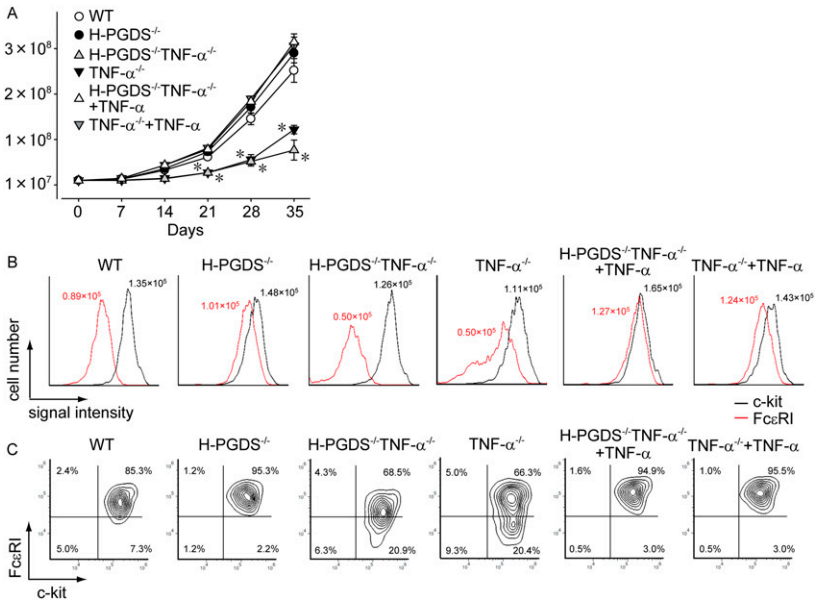

Fig. S3. TNF-α but not PGD_2 is required for IL-3–mediated bone marrow-derived mast cell (BMMC) differentiation and maturation. (*A*) Isolated bone marrow cells were cultured with 5 ng/mL IL-3 and cell numbers were monitored at each time point. In some experiments, 1 ng/mL TNF-α was additionally added ($n = 5$ each; $*^{\dagger}P < 0.05$ compared with WT, H-PGDS$^{-/-}$TNF-α$^{-/-}$, or TNF-α$^{-/-}$). (*B* and *C*) Cell-surface expressions of FcεR1 and c-kit were analyzed by FACS. Representative data from four independent experiments are shown.

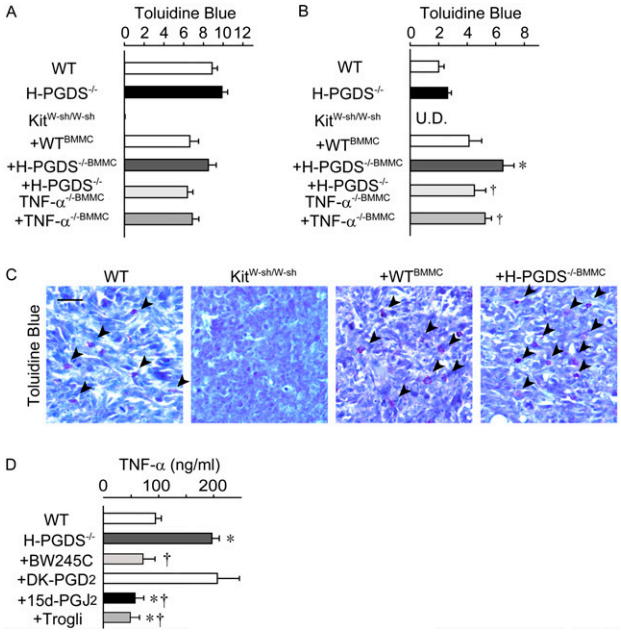

Fig. S4. (*A* and *B*) Mast cell reconstitution in back skin and lung on $Kit^{W\text{-}sh/W\text{-}sh}$ mice. BMMCs were transferred by intradermal and by tail-vein injection into $Kit^{W\text{-}sh/W\text{-}sh}$ mice. Eight weeks after the injection, tissues were dissected and subjected to Toluidine blue staining. The number of metachromatically stained cells were normalized to field area (*A* and *B*, results are expressed as means ± SEM, $n = 4$; $*^{\dagger}P < 0.05$ compared with WT^{BMMC}-reconstituted $Kit^{W\text{-}sh/W\text{-}sh}$ mice or H-$PGDS^{-/-BMMC}$-reconstituted mice, respectively). (*C*) Mast cell reconstitution in tumor on $Kit^{W\text{-}sh/W\text{-}sh}$ mice. BMMCs were transferred into $Kit^{W\text{-}sh/W\text{-}sh}$ mice as mentioned above. Additionally, after LLC transplantation, BMMCs were injected by tail vein every 5 d. Fourteen days after the LLC transplantation, tumors were excised, and processed for Toluidine blue staining (Scale bar, 50 μm). (*D*) H-PGDS deficiency accelerates and D prostanoid agonism or PGJ_2 attenuates TNF-α production of BMMC. BW245C (100 nM), DK-PGD_2 (100 nM), 15d-PGJ_2 (15-deoxy-^{12,14}-PGJ_2; 30 nM), or Troglitazone (300 nM) was treated 10 min before the LPS-stimulation. Twenty-four hours after stimulation with 10 ng/mL LPS, supernatants of BMMC culture were collected and applied to ELISA. Results are expressed as means ± SEM, $n = 4–8$, $*^{\dagger}P < 0.05$ compared with WT or H-$PGDS^{-/-}$, respectively.

Table S1. Primer lists

Name		Sequences
VEGF-A	Sense	TGCACCCACGACAGAAGGA
	Antisense	GTCCACCAGGGTCTCAATCG
bFGF	Sense	GGCTGCTGGCTTCTAAGTGT
	Antisense	TATGGCCTTCTGTCCAGGTC
EGF	Sense	CCCAGGCAACGTATCAAAGT
	Antisense	GGTCATACCCAGGAAAGCAA
Angiopoetin-1	Sense	CCATGCTTGAGATAGGAACCAG
	Antisense	TTCAAGTCGGGATGTTTGATTT
TNF-α	Sense	ACGGCATGGATCTCAAAGAC
	Antisense	CGGACTCCGCAAAGTCTAAG
IL-1β	Sense	AGCTCTCCACCTCAATGGAC
	Antisense	GACAGGCTTGTGCTCTGCTT
IL-6	Sense	TCTCTGGGAAATCGTGGAAA
	Antisense	GATGGTCTTGGTCCTTAGCC
MCP-1	Sense	AATGCTAACGCCACCGAGAG
	Antisense	CCTTGTTCTGCTCCTCATAGTCC
GM-SCF	Sense	TGGTCTACAGCCTCTCAGCA
	Antisense	ATGAAATCCGCATAGGTGGT
TGF-β	Sense	TAGGAAGGACCTGGGTTGGAAG
	Antisense	CGGGTTGTGTTGGTTGTAGAGG
MMP-2	Sense	GACATACATCTTTGCAGGAGACAAG
	Antisense	TCTGCGATGAGCTTAGGGAAA
MMP-9	Sense	AGAAGCAGTCTCTACGGCCG
	Antisense	TGATGGTCCCACTTGAGGCC
COX-2	Sense	TTTGGTCTGGTGCCTGGTC
	Antisense	CTGCTGGTTTGGAATAGTTGCTC
mPGES-1	Sense	ATGAGGCTGCGGAAGAAGG
	Antisense	ATGAGGCTGCGGAAGAAGG
GAPDH	Sense	CCCTGTTGCTGTAGCCGTAT
	Antisense	TGTTCCTACCCCCAATGTGT

MMP, matrix metallopeptidase; mPGES, microsomal PGE_2 synthase.